Methyl Loss Kinetics of Energy-Selected 1,3-Butadiene and Methylcyclopropene Cations

Jeffrey W. Keister and Tomas Baer*

William Rand Kenan, Jr. Laboratories of Chemistry, The University of North Carolina at Chapel Hill, Chapel Hill, North Carolina 27599-3290

Matt Evans and C. Y. Ng

Ames Laboratory, USDOE and Department of Chemistry, Iowa State University, Ames, Iowa 50011

Chia-Wei Hsu

Chemical Sciences Division, Lawrence Berkeley National Laboratory, Berkeley, California 94720

Received: September 20, 1996; In Final Form: November 25, 1996[⊗]

The kinetics of the metastable dissociation of energy-selected 1,3-butadiene and 3-methylcyclopropene cations to form $C_3H_3^+$ (cyclopropenyl cation) and CH_3 have been investigated by threshold photoelectron photoion coincidence (TPEPICO) time-of-flight mass spectrometry, *ab initio* molecular orbital calculations, and RRKM statistical theory. Both the experimental results and the molecular orbital calculations indicate that 1,3-butadiene ions lose CH_3 by first isomerizing to a higher energy structure (3-methylcyclopropene cation) which can rapidly lose CH_3 or isomerize back to the 1,3-butadiene cation. A complete kinetic model of the two-well potential and its three rate constants is necessary to account for the measured dissociation rates as a function of the ion internal energy. At low energies, the dissociation rate is limited by the bond cleavage step, while at higher energies, the bottleneck shifts to the lower energy isomerization step. A fit of calculated RRKM rate constants to the experimental data yields a 0 K isomerization barrier (relative to the 1,3-butadiene ion) of 2.02 ± 0.03 eV and an activation entropy at 600 K of −4 cal K^{-1} mol^{-1}. The entropy of activation for the dissociation step from 3-methylcyclopropene was found to be +7 cal K^{-1} mol^{-1}. 3-Methylcyclopropene was found to have an adiabatic ionization energy of 9.28 ± 0.05 eV and a neutral heat of formation of 273 ± 2 kJ mol^{-1} at 0 K (257 ± 2 kJ mol^{-1} at 298 K). This is the first experimental determination of this value.

Introduction

The methyl loss reaction of $C_4H_6^+$ ions has been extensively investigated.[1−9] Werner and Baer[1] have shown that a number of isomers (1,3- and 1,2-butadiene, 1- and 2-butyne, and cyclobutene) dissociate with identical rate constants, thus demonstrating that these ions rapidly isomerize to the lowest energy 1,3-butadiene ion prior to dissociation. The barrier for isomerization from the butyne ions to 1,3-butadiene ion was found to lie 0.5 eV below the dissociation limit.[2] RRKM calculations of the $C_4H_6^+$ methyl loss rate constant *k(E)* substantially underestimated the experimental values. The first model to provide a reasonable fit to the available *k(E)* data was based on a two-step reaction mechanism in which the rate-determining step was an isomerization to a higher energy (3-methylcyclopropene ion) structure. This model, proposed by Chesnavich and Bowers,[3] lowers the effective energy barrier so that the calculated *k(E)* value can increase to match the experimental rates. A test of this model involves the direct preparation of the higher energy 3-methylcyclopropene cation. For the isomerization step to be rate determining, the dissociation of this ion should be very rapid. Since preliminary tests implied that no isomerization barrier exists, a more detailed analysis was needed. This was undertaken by Jarrold and co-workers, who used a transition state switching model to fit the data.[4]

Although these models have been able to match the magnitude of the experimental rate constants, the fits were not especially good. An important reason for this is the thermal energy distribution of the samples used in the experiments. In this work we have addressed this problem by collecting rate data under both thermal and molecular beam conditions. The temperatures of these two samples are taken into account in the extraction of 0 K rate constant values. In addition, we reexamined the original two-well model and its implications with respect to the 3-methylcyclopropene cation. We have measured the rate constants for this molecular ion and have incorporated these results into a comprehensive model for the dissociation of $C_4H_6^+$ ions. Finally, we have explored the potential energy surface through *ab initio* calculations to obtain geometries, energies, and vibrational frequencies of stable $C_4H_6^+$ structures and the transition states that connect them.

Experimental Setup

Two threshold photoelectron photoion coincidence (TPEPICO) apparatuses were used in this study. The previously described UNC setup[10] was employed with a hydrogen discharge lamp and 1 m monochromator, providing a photon energy resolution of 15 meV, while the recently described TPEPICO setup at the Chemical Dynamics beamline of the Advanced Light Source (ALS)[11] used undulator radiation from the ALS, which was dispersed by a 6.65 m monochromator for a photon energy resolution of 1.3 meV. Because the ring was operated in multibunch mode, the light pulses were separated by only 2.1 ns, providing an effectively continuous light source. The remaining experimental details are very similar. Photoionization takes place in a region of constant 10−20 V/cm electric field, which extracts the ions and electrons in opposite directions. Threshold electrons, selected by a steradiancy analyzer and a hemispherical electrostatic analyzer, with an energy resolution of ∼20 meV at UNC and ∼3.5 meV at ALS, provide the start

* Corresponding author.
[⊗] Abstract published in *Advance ACS Abstracts,* February 15, 1997.

S1089-5639(96)02900-3 CCC: $14.00

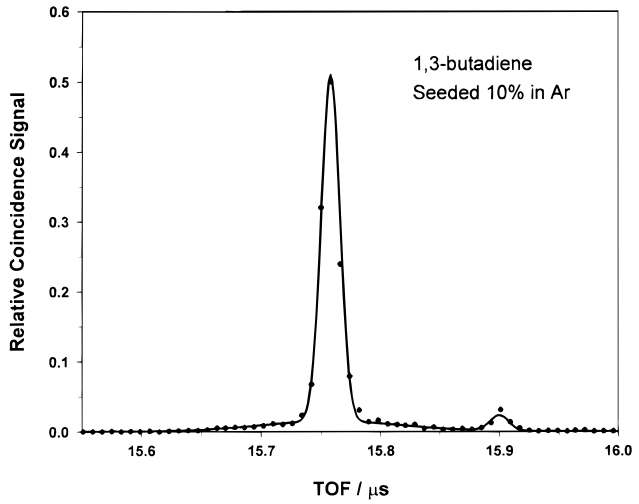

Figure 1. The 1,3-butadiene parent ion TOF peak taken at UNC at the photoionization threshold energy of 9.07 eV. The 20 ns wide peak at 15.76 μs is due to the translationally cold sample in the molecular beam. A much broader 130 ns wide peak, comprising 20% of the total signal, is a result of the thermal background gas in the vacuum chamber. The small peak at 15.9 μs is due to the ^{13}C isotope.

signal for measuring the coincident (energy-selected) ion time-of-flight (TOF) distribution.

The bulk of our rate constant measurements were made using standard two acceleration regions and one drift region TOF setup. However, at low ion energies, where the rate constants are very low, too few daughter $C_3H_3^+$ ions are formed to give a measurable rate constant for the daughter ion TOF peak. Thus, the rate constant was measured at low energies by the use of an additional acceleration region. The additional field was applied 11 cm from the ion detector to separate parent $C_4H_6^+$ ions from daughter ions which have formed in the drift tube, thus giving a second daughter ion peak. The rate constant was then derived from the ratio of peak areas. This method is similar to that employed in some reflectron TOF experiments.[12,13]

Although the sample was expanded in a molecular beam as a seeded 10% mixture in argon, a significant fraction of the ion signal originated from thermal background gas. This is illustrated in Figure 1 for the 1,3-butadiene parent ion TOF distribution obtained at the ionization energy. The narrow part of the peak is due to the molecular beam sample which has been cooled translationally in the direction of ion extraction (perpendicular to the axis of propagation of the molecular beam). The broad part of the peak is due to thermal sample. The data in Figure 1 were obtained at UNC, where we used ~300 Torr backing pressure and one skimmer with differential pumping. This relatively small thermal background signal (~20%) is contrasted with 56% at the ALS, where the backing pressure was ~2 atm and two skimmers were used. We attribute the increased thermal background at the ALS to the lack of nozzle positioning ability. Data were collected for both molecular beam and thermal samples in order to obtain molecular beam spectra which have been corrected for thermal background gas by subtraction.

While the molecular beam gave molecules a very low translational temperature (~5 K) along the ion extraction axis (primarily due to skimming), the internal temperature was significantly higher. The total ro-vibrational energy of 1,3-butadiene at room temperature is 90 meV. The internal energy that remains in the sample after expansion can be readily determined by measuring the shift in the dissociative photoionization onset for molecular beam and thermal samples.[14] This was accomplished by measuring the crossover energy for both thermal and molecular beam samples. Figure 2 shows the shift

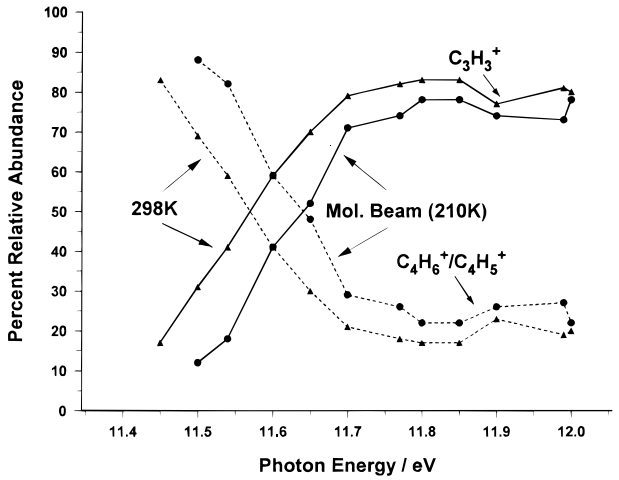

Figure 2. The 298 K and molecular beam breakdown diagrams for the methyl loss reaction of 1,3-butadiene cations collected at UNC. Production of $C_3H_3^+$ is the dominant dissociation channel in this entire energy region, although $C_4H_5^+$ begins to appear in small amounts near 12 eV photon energy.

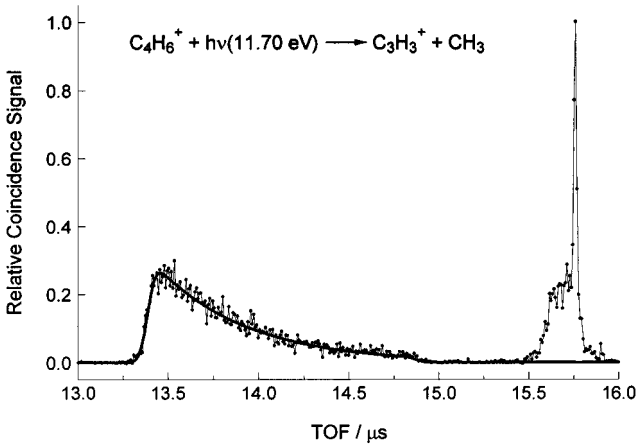

Figure 3. TOF spectrum of jet-cooled 1,3-butadiene at 11.70 eV photon energy. This spectrum has been corrected for thermal background as described in the Experimental Setup section. The broad peak at 15.65 μs is due to $C_3H_3^+$ formed in the drift region.

of 65 meV for the UNC data. Thus, the expansion in the seeded beam removed 65 meV of internal energy. If we assume that the rotations were fully cooled, we find that the vibrational temperature which corresponds to the 25 meV of remaining energy in our 1,3-butadiene sample is 210 K. A similar analysis of the ALS data gave a vibrational temperature of 220 K.

1,3-Butadiene (99+%) was purchased from Matheson. 3-Methylcyclopropene was obtained via the one-step synthesis of Köster et al.[15] The estimated purity of this sample was at least 90%, based upon photoionization mass spectra taken in our laboratory.

Experimental Results

Figure 3 shows a typical TOF distribution of 1,3-butadiene in the energy region just above the dissociation limit. The asymmetric TOF peak (13.5−15 μs) is a result of the $C_4H_6^+$ ions dissociating to produce $C_3H_3^+$ while they are being accelerated in the first acceleration region. The broad shoulder to the left of the sharp parent ion peak at 15.8 μs is due to metastable ions that dissociated in the drift region. These fragment ions arrive slightly ahead of the parent ions because they are more strongly accelerated between the end of the drift region and the ion detector. The heavy solid line is a calculated TOF distribution which is matched to the experimental data using a single, effective ion dissociation rate constant as the

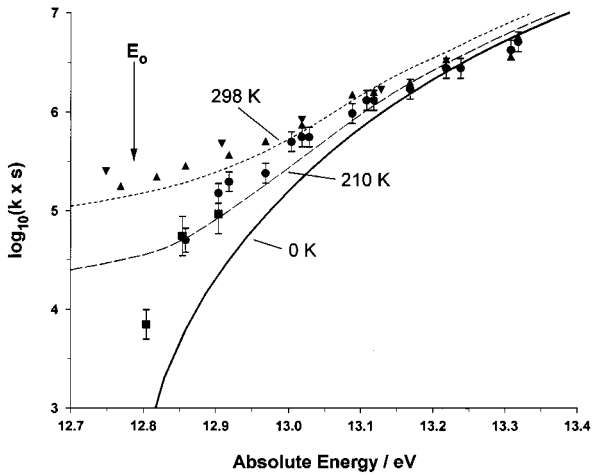

Figure 4. Experimental *k(E)* results (▲, 298 K daughter ion TOF peak shape result; ●, 210 K daughter ion TOF peak shape result; ■, 210 K peak area result; ▼, thermal data from ref 1) plotted with the RRKM curves described in the text. The upper curves are calculated from the lower one using the $C_4H_6^+$ thermal distribution of internal energies at 298 and 210 K, with averaging done as described in the text. The dark solid line is the true 0 K *k(E)* curve.

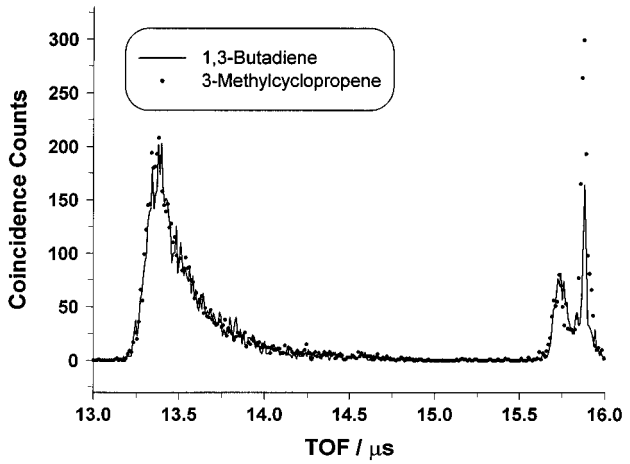

Figure 5. Molecular beam TOF spectra for 3-methylcyclopropene at 10.29 eV photon energy (dots), overlaid with the molecular beam TOF spectra for 1,3-butadiene at 11.80 eV photon energy. These spectra were not corrected for thermal background. The only observable difference is an extra 9% parent ion signal for the 3-methylcyclopropene spectrum, which we attribute to an impurity of lower energy C_4H_6 isomers in the sample used.

fitting parameter. This theoretical distribution was obtained by convoluting a TOF simulation with a Gaussian function in the TOF domain to match the natural width of the daughter ion peak, which is a result of the parent ion width, broadened by the kinetic energy released in the dissociation. The rate constant at this photon energy was found to be 5.6×10^5 s^{-1}. Similar data were collected at other ion internal energies. When rate constants are measured in this way (from the shape of the asymmetric daughter ion TOF peak), the lowest measurable rate constant value is about 10^4 s^{-1}. This is because it only takes 5.29 μs for the parent $C_4H_6^+$ ion to reach the drift tube, so that at a rate constant of 10^4 s^{-1} only 5% of the ions dissociate in the acceleration region (in the UNC apparatus). The remaining 95% of the ions contribute to the parent ion peak. The measurable rate constant range can be extended below 10^4 s^{-1} by counting the number of ions that dissociate in the drift tube (between 5.29 and 15.75 μs in the UNC apparatus). Thus, at the lowest energies, the rate constants were instead derived from the previously mentioned peak area ratios using the additional acceleration region at the end of the drift region. All of the derived rate constants for the room temperature and 210 K molecular beam data are displayed in Figure 4 (points).

The rate constant data in Figure 4 show a peculiar leveling off at low energies, especially for the 298 K case. This is a result of the thermal internal energy distribution. As the threshold energy of 12.786 eV is approached, the dissociation rate decreases dramatically. Ions with very low dissociation rate constants are not detected as daughter ions but as parent ions because they enter the drift tube at 5.29 μs, long before the ions have a chance to dissociate. This is related to the well-known kinetic shift.[17,18] Thus, at photon energies close to threshold, the very low-energy ions do not dissociate. On the other hand, molecules with significant thermal internal energy may have ion energies in excess of the dissociation threshold. They will fragment with rates significantly higher than the low energy ions and produce more daughter ion signal. Thus, the apparent leveling off of the dissociation rate constant as the threshold photon energy is approached is a direct result of the thermal internal energy in the room temperature and molecular beam samples.

The effect of the thermal distribution was taken into account by convoluting the 298 and 210 K vibrational energy distributions with an assumed 0 K *k(E)* curve (lower solid line, Figure 4). The thermal distribution of energies was taken into account by finding an "effective" dissociation rate constant, obtained from a linear combination of properly weighted decay curves. That is:

$$k_{\text{eff}}(E)\mathrm{e}^{-k_{\text{eff}}(E)t} \approx \int_0^\infty P(\epsilon)\, k(E+\epsilon)\mathrm{e}^{-k(E+\epsilon)t}\, \mathrm{d}\epsilon \qquad (1)$$

where $P(\epsilon)$ is the normalized thermal energy distribution function at 298 or 210 K, *k(E)* is the true (0 K) dissociation rate constant, and k_{eff} is the effective decay rate constant which reproduces the measured TOF distributions as a function of energy. Although the sum of the exponential decays is not precisely an exponential function, it is very close to one. This convolution produces the upper curves in Figure 4; the true 0 K dissociation rate constant is given by the lower solid line. While this thermal correction is most important near threshold, the effect persists at higher energies where the 298 and 210 K rate constants are shifted from the 0 K values by the average 90 and 25 meV of thermal energy. Such an analysis only applies to the rate data derived from the asymmetrically broadened daughter ion TOF peaks. The rate constants found from the ratio of peak areas have a different correction because of the longer ion residence times. The 0 K *k(E)* curves were obtained from the RRKM rate calculations discussed in more detail in the RRKM and Kinetics Modeling section.

A similar set of data were collected for 3-methylcyclopropene. These rates were also found to be slow. An example is shown in Figure 5, where the 3-methylcylopropene data at a photon energy of 10.29 eV (points) are plotted on the same graph as the 1,3-butadiene data at a photon energy of 11.80 eV (solid line). The photon energies are different because the neutral molecules have different heats of formation. The exact agreement between the dissociation rate constants of the two ions at these two photon energies (as well as other sets of energies) indicates that the total ion energy relative to the product $C_3H_3^+ + CH_3$ energy is the same. Thus, the difference in the photon energies required to give similar dissociation rate constants for the two ions is the difference in neutral heats of formation. We use this to obtain a rather precise measure of the 3-methylcyclopropene standard heat of formation at 298 K of 257 ± 2 kJ mol^{-1}. This is the first experimental value for this heat of formation. It is somewhat larger than the 248 kJ mol^{-1} value given by Benson's additivity scheme.[16]

The similarity of the 1,3-butadiene and 3-methylcyclopropene rate constants clearly indicates that at most of these energies the 3-methylcyclopropene ion preferentially isomerizes to the lower energy 1,3-butadiene isomer rather than directly producing the bond cleavage products. The TPEPICO TOF data for 3-methylcyclopropene and 1,3-butadiene ions were identical at all energies investigated, and in all cases, the data could be fit with a single-exponential decay rate. However, it should be pointed out that, in order to observe a rapid, direct dissociation which is characterized by a narrow, symmetric daughter ion TOF peak, the fraction of the ions dissociating rapidly would have to be at least 20% at observed rates of 6×10^5 s^{-1} or less. This is significant in the analysis and will be discussed in detail in the RRKM and Kinetics Modeling section.

The UNC apparatus was also used to measure an ionization energy (IE) for 3-methylcyclopropene. We found a rather broad TPES peak (with fwhm of ~650 meV) centered at a photon energy of 9.73 ± 0.05 eV and an onset near 9.28 eV. The difference between the vertical and adiabatic ionization energies matches the *ab initio* molecular orbital calculations described in the next section.

Ab Initio Investigation

As pointed out in the Introduction, the proposed mechanism for the methyl loss reaction of the 1,3-butadiene cation is not a simple bond dissociation step. Rather, the parent ion must first isomerize to a methyl functional cyclic structure from which the cyclopropenyl ion and CH_3 products can form. We have thus carried out a series of *ab initio* molecular orbital calculations to study the reaction path for this dissociation.

The *ab initio* molecular orbital calculations in this study were performed using the Gaussian 92 package[19] on a Convex 3840 supercomputer at UNC. Several levels of theory were used, from UHF/6-31g* to MP2/6-311g**. The highest level calculations were obtained using MP2/6-31g* geometry optimizations and frequency sets (corrected by 0.95[20]), with single-point energies calculated from these geometries using MP2/6-311g**. The UHF frequencies were corrected by a factor of 0.90.[20] All transition state (TS) geometries were tested using the intrinsic reaction coordinate procedure of Gaussian 92.

Although the 3-methylcyclopropene ion is the logical high-energy intermediate for the dissociation of $C_4H_6^+$ ions to the $C_3H_3^+$ cyclopropenyl ion, the *ab initio* molecular orbital calculations revealed a rather complicated reaction path with several stable wells along the way to products (see Figure 6). The calculated energy values are listed in Table 1. A major surprise was the discovery of two different c-C_3H_3−CH_3^+ structures. The lower energy isomer corresponds to direct ionization of the neutral 3-methylcyclopropene. Stretching the methyl−ring bond distance reveals a TS that connects the 3-methylcyclopropene ion to a configuration best thought of as an "associated complex" of the methyl radical and cyclopropenyl cation dissociation products. This minimum-energy structure has a methyl−ring C−C bond distance of 2.9 Å, which is rather large compared to the 1.5 Å distance found in the 3-methylcyclopropene ion. In addition, the normal modes for this species can be identified with those for the c-$C_3H_3^+$ and CH_3 products plus the six remaining interproduct modes which have comparatively low vibrational frequencies (see Table 2).

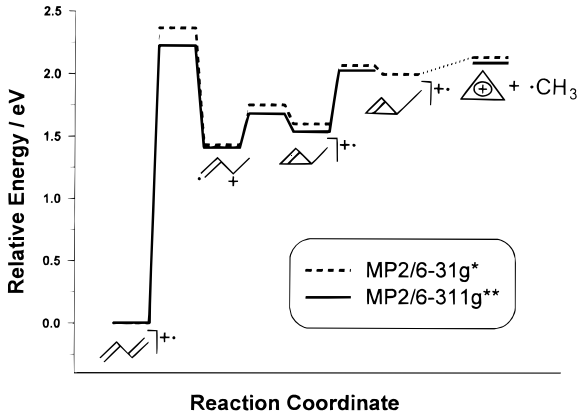

Figure 6. Energies of various $C_4H_6^+$ structures along the reaction path as calculated by the indicated Gaussian 92 *ab initio* MO methods. 1,3-Butadiene is on the left, and products are on the right. The first barrier is the largest and corresponds to 1,4-hydrogen atom transfer.

The reaction path that connects the 3-methylcyclopropene ion to the 1,3-butadiene ion also holds interesting subtleties. These species are separated by hydrogen transfer (methyl formation) and cyclization (ring forming). The lowest energy path that was found to connect them passes through an intermediate minimum-energy structure which contains the methyl functionality but remains a straight-chain isomer. The 1,3-diradical−butene ion is formed in its *cis* conformation via 1,4-hydrogen transfer from the *cis*-1,3-butadiene ion. This species is connected to the 3-methylcyclopropene ion via a simple C−C bond forming step. This mechanism is supported by recent unpublished work of Čársky et al.[21]

The relative energies of these minimum-energy and TS structures (Figure 6) indicate that the isomerization bottleneck is likely to correspond to hydrogen transfer rather than cyclization. In addition, we find justification for using the barrier which separates the 3-methylcyclopropene ion and the associated complex as a good approximation to the dissociation TS.

It is evident that the calculated dissociation energies of 2.129 and 2.085 eV, which are based on the energy difference between the calculated 1,3-butadiene ion and the dissociation products, do not match the known value of 2.40 eV (see Table 3). The latter energy is determined by combining a G2 *ab initio* calculation of the c-$C_3H_3^+$ heat of formation (based on atomi-

TABLE 1: *Ab Initio* Energy Results[a]

species	level			experiment
	UHF/6-31g*//UHF/6-31g*	MP2/6-31g*//MP2/6-31g*	MP2/6-311g**//MP2/6-31g*	
s-trans-1,3-butadiene cation	0	0	0	0
s-cis-1,3-butadiene cation	0.175	0.182		
1,4 hydrogen transfer TS	2.829	2.364	2.223	2.02 ± 0.03[b]
s-trans-n-$(CH)_3CH_3^+$	1.264	1.429	1.405	
s-*cis*-*n*-$(CH)_3CH_3^+$	1.341	1.541		
cyclization TS	2.401	1.749	1.680	
3-methylcyclopropenyl cation	2.344	1.597	1.534	1.74 ± 0.20[b]
methyl loss TS	2.606	2.064	2.023	
associated complex		1.994		
products: cyclopropenyl cation + $^{\bullet}CH_3$	2.129	2.129	2.085	2.40 ± 0.01[c]

[a] Relative energies in electronvolts, corrected for zero point vibrational energy. [b] This work. [c] Derived from ref 22−26.

TABLE 2: *Ab Initio* MP2/6-31g* Frequency Results[a]

species	vibrational frequencies, cm^{-1}
s-trans-1,3-butadiene cation	175, 280, 448, 506, 540, 890, 921, 984, 991, 1049, 1051, 1230, 1258, 1273, 1323, 1470, 1487, 1617, 3066, 3069, 3082, 3088, 3178, 3178
1,4 hydrogen transfer TS, connecting *s-cis*-1,3-butadiene cation with *s-cis-n*-$(CH)_3CH_3^+$ ion	292, 501, 532, 664, 819, 838, 921, 965, 1019, 1066, 1089, 1204, 1228, 1307, 1372, 1453, 1507, 1749, 3000, 3086, 3099, 3105, 3116, 1718i
s-*trans-n*-$(CH)_3CH_3^+$ cation	110, 148, 286, 485, 639, 800, 886, 904, 969, 1075, 1154, 1231, 1264, 1327, 1397, 1410, 1479, 1546, 2903, 2955, 3053, 3061, 3089, 3147
cyclization TS connecting *s-trans-n*-$(CH)_3CH_3^+$ cation with 3-methylcyclopropene cation	122, 313, 366, 392, 701,807, 832, 890, 979, 1029, 1114, 1182, 1354, 1372, 1432, 1456, 1730, 2937, 3010, 3062, 3079, 3100, 3251, 267i
3-methylcyclopropene cation	148, 224, 330, 427, 624, 772, 791, 835, 879, 932, 976, 1010, 1076, 1252, 1370, 1435, 1449, 1651, 2942, 2965, 3033, 3080, 3139, 3196
TS connecting 3-methylcyclopropene cation with associated complex c-$C_3H_3^+$−$^{\bullet}CH_3$	64, 158, 229, 422, 434, 738, 891, 895, 931, 932, 956, 1004, 1295, 1260, 1404, 1406, 1574, 3022, 3164, 3168, 3197, 3199, 3207, 202i
associated complex c-$C_3H_3^+$−$^{\bullet}CH_3$	27, 69, 81, 154, 229, 232, 707, 786, 903, 912, 918, 941, 1006, 1269, 1277, 1407, 1407, 1589, 3032, 3163, 3176, 3205, 3207, 3217
cyclopropenyl cation c-$C_3H_3^+$	720, 913, 913, 948, 948, 1007, 1277, 1277, 1592, 3159, 3159, 3205
methyl radical $^{\bullet}CH_3$	381, 1407, 1407, 3059, 3238, 3238

[a] Frequencies are corrected by multiplication by a factor of 0.95.

TABLE 3: Thermochemical Values

species	IE/eV	$\Delta H_f^0{}_{(298\ K)}$/ kJ mol^{-1}	$\Delta H_f^0{}_{(0\ K)}$/ kJ mol^{-1}
1,3-butadiene	9.070 ± 0.004[a]	110 ± 1[b]	127[c]
1,3-butadiene cation		985[d]	1002[d]
cyclopropenyl cation		1080[e]	1085[e]
methyl radical		145.8[f]	149.0[f]
3-methylcyclopropene	9.14 ± 0.09[g]	248[i]	264[i,j]
	9.28 ± 0.05[h]	257 ± 2[h]	273 ± 2[h,j]
3-methylcyclopropene cation		1132[d,g,i]	1148 ± 5[d,g,i,j]
		1153 ± 5[d,h]	1169 ± 5[d,h,j]

[a] Reference 22. [b] Reference 23. [c] Derived from the 298 K value using vibrational frequencies from ref 24. [d] Sum of IE and neutral heat of formation. [e] Reference 26. [f] Reference 25. [g] Reference 5. [h] This work. [i] Calculated using the method of Benson (ref 16). [j] Derived from the 298 K heat of formation using vibrational frequencies calculated in this work.

zation energies) by Wong and Radom[26] with the experimental heats of formation for the 1,3-butadiene ion and CH_3 radical. The agreement between the 298 K $C_3H_3^+$ heats of formation obtained from G2 theory (1080 kJ/mol[26]) and experiment (1075 kJ/mol[27]) makes the uncertainty in the dissociation limit rather small. We thus use this dissociation limit in the RRKM rate constant calculations. The discrepancy between this value and our calculations indicates the limited energy accuracy of our lower level of theory. In light of this limitation, our calculated energy of the transition state between the 1,3-butadiene ion and the 1,3-diradical butene ion cannot be expected to be very accurate either.

As pointed out in the Results section, the first band of the 3-methylcyclopropene TPES is characterized by a broad peak for which the adiabatic ionization energy is difficult to assign. On the other hand, the vertical IE at the peak maximum is readily located at 9.73 ± 0.05 eV. The expected shift between the adiabatic and vertical IE of 3-methylcyclopropene was calculated by comparing the (vibrationless) energy of the 3-methylcyclopropene ion optimized at MP2/6-31g* with the MP2/6-31g* single-point energy of the 3-methylcyclopropene ion at the optimized 3-methylcyclopropene (neutral) geometry. The shift in the IE values was calculated to be a rather significant 0.453 eV, which matches the experimental determination of 0.45 $\pm$ 0.05 eV. In fact, the optimized ion and neutral geometries are strikingly different. Although the neutral has a plane of symmetry running perpendicular to the ring that includes the 3 and 4 carbons (and one hydrogen of each), the ion is skewed at the 3 carbon. This difference in geometry can be expected to give rise to a broad TPES peak, which is observed experimentally.

RRKM and Kinetics Modeling

The statistical RRKM theory[28] was used to calculate the 0 K rate constants. The RRKM expression for an individual reaction step as a function of energy is given by

$$k(E) = \frac{\sigma N^{\ddagger}(E - E_0)}{h\rho(E)} \qquad (2)$$

where E is the energy above the reactant, E_0 is the TS energy, $N^{\ddagger}(E - E_0)$ is the number of internal states in the transition state between 0 and $E - E_0$, $\rho(E)$ is the density of internal states in the reactant, h is the Planck constant, and σ is the symmetry factor (ratio of reactant to TS symmetry numbers), which is used to compensate for the neglect of rotational symmetry in the calculation of densities and sums of states.

The simplest model for the 1,3-butadiene ion dissociation is a single-step reaction through a loose dissociation transition state. If we use the calculated vibrational frequencies of 1,3-butadiene and the "methyl loss" dissociation TS (Table 2), along with the known thermochemical dissociation threshold energy E_0 of 2.40 $\pm$ 0.01 eV, we can match the magnitude of the experimental *k(E)* values by loosening the transition state from +6 eu (cal K^{-1} mol^{-1} at 600 K) to +8 eu. This is achieved by multiplying the lowest five TS vibrational frequencies by a scaling factor of 0.8. This result matches the experimental *k(E)* curve near threshold but fails at higher energies. Such a theoretical curve is characteristic of a loose transition state and has a relatively steep slope. The experimental data, on the other hand, are characterized by a steep slope at low energies and a shallow slope at higher energies, indicative of a tight TS.

The switching from a loose to a tight TS indicates that the reaction rate is determined by a two-well potential energy surface as shown in Figure 7 in which the 1,3-butadiene ion first rearranges to a higher energy structure which "looks like" the products. This is precisely the model that was proposed by Chesnavich and Bowers.[3] However, the difference is that, with the proper analysis of the rate data which includes the effect of the thermal energy distribution, the switching from the loose TS (rate constant k_1) to the tight (rate constant k_3) occurs at much higher energies than proposed by Chesnavich and Bowers.

In order to fit the observed 3-methylcyclopropene ion rate constant *k(E)* over the whole energy range, it is necessary to consider the competition between isomerization (k_2) and dissociation (k_1). For a reaction scheme as shown in Figure 7, the 1,3-butadiene ion should decay with a slow single-exponential decay rate, while the methyl cyclopropene ion should decay by a two-component decay rate in which the two rates are given

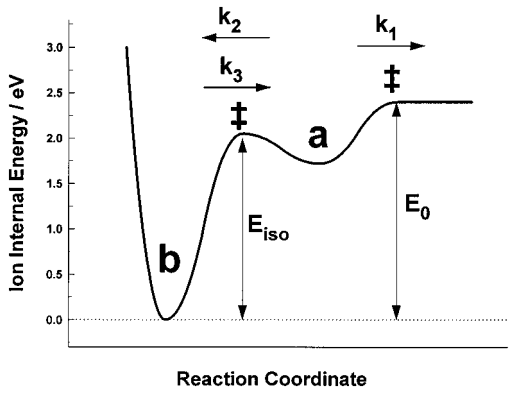

Figure 7. Two-well potential energy surface used in modeling the observed reaction rates. The **a** well is the 3-methylcylopropene cation (and 1,3-diradical butene cation), and the **b** well is 1,3-butadiene ion. The energy of the isomerization TS is derived from fitting the experimental rate constant data.

by

$$k_{\text{fast,slow}} = k_{\pm} = 1/2(k_1 + k_2 + k_3 \pm \sqrt{(k_1 + k_2 + k_3)^2 - 4k_1k_3}) \quad (3)$$

The percent fast component which arises when the potential well **a** is first prepared is

$$\% \text{ fast} = 100 \times \frac{k_1 - k_{\text{slow}}}{k_{\text{fast}} - k_{\text{slow}}} \quad (4)$$

Features of the 1,3-butadiene system permit simplification of eqs 3 and 4. Because of the relatively high energy of the 3-methylcyclopropene ion, its concentration is relatively constant (it is depleted as soon as it is formed) so that the steady state approximation can be applied to the **a** isomer. This is equivalent to stating that k_3 is negligible compared to k_1 and k_2. This approximation was tested and found to be valid for all cases in which the complete formulation matches the data. The results of this approximation are

$$k_{\text{fast}} = k_1 + k_2 \quad (5)$$

$$k_{\text{slow}} = \frac{k_1k_3}{k_1 + k_2} \quad (6)$$

and the corresponding percent fast component seen from **a** is

$$\% \text{ fast} = 100 \times \frac{k_1}{k_1 + k_2} \quad (7)$$

The observable rate constant in our experiment is k_{slow} which, if written in terms of the RRKM variables $N^{\ddagger}$ and ρ, is

$$k_{\text{slow}} = \frac{\sigma_1 N_{\text{diss}}{}^{\ddagger}(E - E_0)\sigma_3 N_{\text{iso}}{}^{\ddagger}(E - E_{\text{iso}})}{h\rho_{\text{b}}(E)(\sigma_1 N_{\text{diss}}{}^{\ddagger}(E - E_0) + \sigma_2 N_{\text{iso}}{}^{\ddagger}(E - E_{\text{iso}}))} \quad (8)$$

For the $C_4H_6^+$ system, σ_1 and σ_2 are taken to be 1 and σ_3 is 2 since 1,3-butadiene has S_2 symmetry. From this equation it is clear that the energy and entropy of the intermediate have become irrelevant because k_1 and k_2 all have the same $h\rho_{\text{a}}$ denominator. Thus, the model implies that the experimental evidence is unable to shed any light on the nature of the **a** well. As a result, the **a** well, in which we include both the 3-methylcyclopropene ion and the linear $(CH)_3CH_3^+$, cannot be assigned to one or the other species.

Equation 8 can be further simplified when there are several orders of magnitude difference between $\sigma_1 N_{\text{diss}}{}^{\ddagger}$ and $\sigma_2 N_{\text{iso}}{}^{\ddagger}$. Near threshold, $N_{\text{diss}}{}^{\ddagger}$ approaches unity. As a result, the overall rate constant simplifies to

$$k_{\text{slow}}(E) = \frac{\sigma_1\sigma_3 N_{\text{diss}}{}^{\ddagger}(E - E_0)}{\sigma_2 h\rho_{\text{b}}(E)} \quad (9)$$

This low-energy limit is essentially a single-well model in which dissociation is rate determining. At high energies, $N_{\text{diss}}{}^{\ddagger}$ outweighs $N_{\text{iso}}{}^{\ddagger}$ because it is a looser transition state with more low vibrational frequencies. As a result, the overall rate constant becomes

$$k_{\text{slow}}(E) = \frac{\sigma_3 N_{\text{iso}}{}^{\ddagger}(E - E_0)}{h\rho_{\text{b}}(E)} \quad (10)$$

This high-energy limit is k_3. This is the case assumed by Chesnavich and Bowers in their attempt to fit the 298 K data at low energies where the slope of *k(E)* is rather small.

The rate data were fit using the complete two-well kinetics model (eq 3) by fixing E_0 at 2.40 eV and setting the entropy of the dissociation transition state to +7 eu (lowest five TS frequencies lowered by 10%). The isomerization TS (hydrogen transfer) frequencies were fixed at the calculated values while the energy of the isomerization TS was varied until a good fit was found between the experiment and calculation (solid lines in Figure 4). The calculated fraction of fast component expected from the 3-methylcyclopropene ion well is shown in Figure 8. We found it possible to simultaneously match the experimental rate constants and keep the amount of direct dissociation below the experimental measurement limit. Specifically, at a 0 K rate constant of 4×10^5 s^{-1} (corresponding to an observed 210 K rate constant k_{eff} of 6×10^5), the percent fast is about 15%, which is below the 20% minimum required for experimental observation. In addition, the crossing of the k_1 and k_2 rate constant curves near 0.6 eV internal energy is the point at which the reaction bottleneck gradually switches from a loose dissociation TS at low energies to a tight isomerization TS at high energies. At this point, the fraction of 3-methylcyclopropene ions dissociating with the fast rate constant reaches 50%. Within a broad energy range of this point, the competition between isomerization and dissociation is quite significant. As a result, the k_{slow} value does not reach the high-energy limit of k_3 in our energy range. The value of E_{iso} which gave a good fit was 2.02 ± 0.03 eV.

Thus, we reconcile the fact that the 1,3-butadiene and 3-methylcyclopropene ion dissociation rates are identical with no observable fast component for the latter. At low energies, the 3-methylcyclopropene ion readily isomerizes ($k_2 \gg k_1$), and dissociation is rate determining. At higher energies, isomerization becomes rate limiting, but the slow rate constant is too high to be experimentally distinguished from the fast one. This is illustrated quantitatively in Figure 8, where the isomerization rate constant, k_2, is shown to be much greater than the dissociation rate constant, k_1, over most of the energy range investigated. This is a type of transition-state switching model[31,32] whose form is encapsulated in eq 8. Although it is safe in this case to apply the steady state approximation, we are not justified in extending this approximation to either the high- or low-energy limiting cases for the whole range of experimental data.

Conclusion

The flat *k(E)* curve we observe experimentally is due to a combination of the thermal internal energy of the 1,3-butadiene

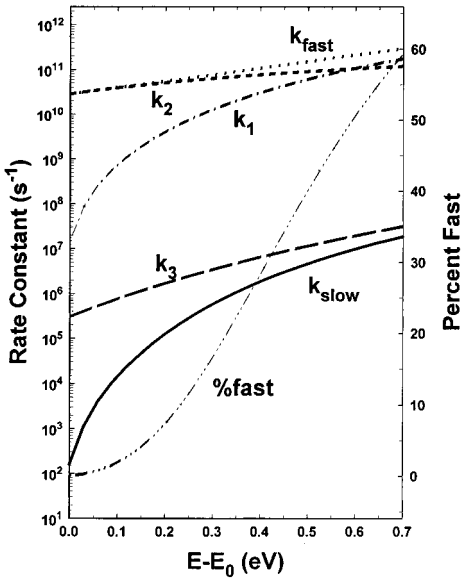

Figure 8. Individual rate constants for the two-well model obtained from the RRKM analysis. Note that, at the energies for which k_{slow} is less than 4×10^5, the fraction of fast component is unmeasurable (~15%).

sample and the reaction being limited at high energies by a tight isomerization step. When the internal temperature is accounted for, we find that the reaction rate is limited by dissociation for the lowest experimental energies. At energies greater than 0.6 eV above the dissociation limit, isomerization becomes rate limiting. The 3-methylcyclopropene cation also gives a slow methyl loss rate constant despite the low barrier to dissociation (0.67 eV). Thus, isomerization (k_2) is competitive with dissociation (k_1) from 3-methylcyclopropene cation in this energy range. A two-well model for $C_4H_6^+$ ions, based in part on *ab initio* calculations, predicts the correct slope for the *k(E)* curve. The 1,3-butadiene ion and the 3-methylcyclopropene ion are connected by a tight isomerization transition state, and although only the 3-methylcyclopropene ion can directly produce methyl loss products, it is more likely to instead isomerize at these energies.

The two-well model employed in this work is obviously simpler than the *ab initio* study implies. We suggest that the isomerization TS in our two-well model corresponds to 1,4-hydrogen transfer, since this configuration has the largest energy of all the transition states found in the *ab initio* study. Because the calculated results are independent of the **a** well energy, the identity of the **a** isomer could be either the 3-methylcyclopropene ion or the 1,3-diradical butene ion. However, the similarity in energy of these species and the low barrier which separates them allows us to treat them together as one potential energy well.

Thus, the Chesnavich−Bowers mechanism of dissociation of the 1,3-butadiene ion through the 3-methylcyclopropene ion is in fact confirmed, in spite of the slow dissociation from the 3-methylcyclopropene ion. We estimate that at most of our energies isomerization prevails over direct dissociation as the dominant pathway from the 3-methylcyclopropene ion. At higher energies, the isomerization TS becomes the relevant bottleneck for 1,3-butadiene and contributes to the shallow *k(E)* curve, although the fast component signal at these energies is experimentally indistinguishable from the slow component signal.

The adiabatic and vertical IE's of 3-methylcyclopropene were measured (9.28 ± 0.05 and 9.73 ± 0.05 eV, respectively), and the difference agrees with the *ab initio* calculation. The observed rate constants for 3-methylcyclopropene matched the 1,3-butadiene values when 3-methylcyclopropene ions were prepared with 1.52 ± 0.02 eV less photon energy. Adding this energy difference to the literature value for 1,3-butadiene ΔH_f(298 K) of 110 kJ mol^{-1} [23] leads to a ΔH_f°(298 K) for 3-methylcyclopropene of 257 ± 2 kJ mol^{-1} and ΔH_f°(0 K) of 273 ± 2 kJ mol^{-1}. This gives a ΔH_f°(0 K) for the 3-methylcyclopropene ion of 1169 ± 5 kJ mol^{-1}. Our RRKM model also gives us the parameters $E_{iso} = 2.02 \pm 0.03$ eV, $\Delta S_{iso}^{\ddagger} = -4 \pm 1$ cal K^{-1} mol^{-1} at 600 K, and $\Delta S_{diss}^{\ddagger} = +7 \pm 1$ cal K^{-1} mol^{-1} at 600 K.

Acknowledgment. We gratefully acknowledge the support of the Department of Energy. We thank Leo Radom and Petr Čársky for allowing us to refer to their unpublished calculations. We also thank the North Carolina Supercomputer Center for a generous grant of computer time.

References and Notes

(1) Werner, A. S.; Baer, T. *J. Chem. Phys.* **1975**, *62*, 2900.
(2) Bunn, T. L.; Baer, T. *J. Chem. Phys.* **1986**, *85*, 6361.
(3) Chesnavich, W. J.; Bowers, M. T. *J. Am. Chem. Soc.* **1977**, *99*, 1705.
(4) Jarrold, M. F.; Bass, L. M.; Kemper, P. R.; vanKoppen, P. A. M.; Bowers, M. T. *J. Chem. Phys.* **1983**, *78*, 3756.
(5) Russell, D. H.; Gross, M. L.; vanderGreef, J.; Nibbering, N. M. M. *J. Am. Chem. Soc.* **1979**, *101*, 2086.
(6) Sellers-Hann, L.; Krailler, R. E.; Russell, D. H. *J. Chem. Phys.* **1988**, *89*, 889.
(7) Bombach, R.; Dannacher, J.; Stadelmann, J. P. *J. Am. Chem. Soc.* **1983**, *105*, 1824.
(8) Dannacher, J.; Flamme, J.; Stadelmann, J.; Vogt, J. *Chem. Phys.* **1980**, *51*, 189.
(9) Baer, T. *J. Electron Spectrosc. Relat. Phenom.* **1979**, *15*, 225.
(10) Booze, J. A.; Baer, T. *J. Chem. Phys.* **1993**, *98*, 186.
(11) Mayer, P. M.; Keister, J. W.; Baer, T.; Evans, M.; Ng, C. Y.; Hsu, C. *J. Phys. Chem.*, in press.
(12) Kuhlewind, H.; Kiermeier, A.; Neusser, H. J. *J. Chem. Phys.* **1986**, *85*, 4427.
(13) Stanley, R. J.; Cook, M.; Castleman, A. W. *J. Phys. Chem.* **1990**, *94*, 3668.
(14) Weitzel, K. M.; Booze, J. A.; Baer, T. *Chem. Phys.* **1991**, *150*, 263.
(15) Koester, R.; Arora, S.; Binger, P. *Angew. Chem., Int. Ed. Engl.* **1970**, *9*, 810.
(16) Benson, S. W. *Thermochemical Kinetics*; John Wiley & Sons: New York, 1976.
(17) Chupka, W. A. *J. Chem. Phys.* **1959**, *30*, 191.
(18) Lifshitz, C. *Mass Spectrom. Rev.* **1982**, *1*, 309.
(19) Frisch, M. J.; Trucks, G. W.; Head-Gordon, M.; Gill, P. M. W.; Wong, M. W.; Foresman, J. B.; Johnson, B. G.; Schlegel, H. B.; Robb, M. A.; Replogle, E. S.; Gomperts, R.; Andres, J. L.; Raghavachari, K.; Binkley, J. S.; Gonzalez, C.; Martin, R. L.; Fox, D. J.; Defrees, D. J.; Baker, J.; Stewart, J. J. P.; Pople, J. A. *GAUSSIAN 92, Revision A*; Gaussian Inc.: Pittsburgh, PA, 1992.
(20) Pople, J. A.; Scott, A. P.; Wong, M. W.; Radom, L. *Isr. J. Chem.* **1993**, *33*, 345.
(21) Čársky, P.; Ingr, M.; Chval, Z.; Bally, T. Proceedings of the 4th World Congress of Theoretically Oriented Chemists, 1996.
(22) Mallard, W. G.; Miller, J. H.; Smyth, K. C. *J. Chem. Phys.* **1983**, *79*, 5900.
(23) Pedley, J. B.; Naylor, R. D.; Kirby, S. P. *Thermochemical Data of Organic Compounds*; Chapman and Hall: London, 1986.
(24) Shimanouchi, T. *Tables of Molecular Vibrational Frequencies*; Natl. Stand. Ref. Data. Ser. (NBS) No. 39: U.S. Government Printing Office: Washington, DC, 1972.
(25) Heneghan, S. P.; Knoot, P. A.; Benson, S. W. *Int. J. Chem. Kinet.* **1981**, *13*, 677.
(26) Wong, M. W.; Radom, L. Unpublished results, 1996.
(27) Lias, S. G.; Bartmess, J. E.; Liebman, J. F.; Holmes, J. L.; Levin, R. D.; Mallard, W. G. *Gas Phase Ion and Neutral Thermochemistry, J. Phys. Chem. Ref. Data Vol. 17, Suppl. 1*; NSRDS: U.S. Government Printing Office: Washington, DC, 1988.
(28) Baer, T.; Hase, W. L. *Unimolecular Reaction Dynamics: Theory and Experiments*; Oxford: New York, 1996.
(29) Baer, T.; Brand, W. A.; Bunn, T. L.; Butler, J. J. *Faraday Discuss.* **1983**, *75*, 45.
(30) Duffy, L. M.; Keister, J. W.; Baer, T. *J. Phys. Chem.* **1995**, *99*, 17862.
(31) Lifshitz, C.; Louage, F.; Aviyente, V.; Song, K. *J. Phys. Chem.* **1991**, *95*, 9298.
(32) Chesnavich, W. J.; Bass, L.; Su, T.; Bowers, M. T. *J. Chem. Phys.* **1981**, *74*, 2228.